

Lipid biomarkers and metal pollution in the Holocene record of Cartagena Bay (SE Spain): Coupled natural and human induced environmental history in Punic and Roman times

José E. Ortiz[1], Trinidad Torres[1], Yolanda Sánchez-Palencia[1], Milagros Ros[2], Sebastián Ramallo[2], Ignacio López-Cilla[3], Luis A. Galán[3], Ignacio Manteca[4], Tomás Rodríguez-Estrella[4], Ana Blázquez[5], Ángeles Gómez-Borrego[6], Blanca Ruiz-Zapata[7], María José Gil[7]

[1] Laboratorio de Estratigrafía Biomolecular. E.T.S.I. Minas y Energía de Madrid, Universidad Politécnica de Madrid. C/ Ríos Rosas 21. 28003-Madrid. joseeugenio.ortiz@upm.es, trinidad.torres@upm.es, yolanda.sanchezpalencia@upm.es.

[2] Departamento de Prehistoria, Arqueología, Historia Antigua, Historia Medieval y Ciencias y Técnicas Historiográficas, Universidad de Murcia. C/ Santo Cristo, 1. 30001-Murcia. milaros@um.es, sfra@um.es.

[3] Departamento de Infraestructura Geocientífica y Servicios, IGME. C/Ríos Rosas 23. 28003-Madrid. i.lopezcilla@gmail.com, l.galan@igme.es.

[4] Departamento de Ingeniería Minera, Geológica y Cartográfica, Universidad Politécnica de Cartagena. Paseo Alfonso XIII, 52. 30203-Cartagena. nacho.manteca@upct.es, tomasrestrella@hotmail.com.

[5] Institute of Environment and Marine Science Research (IMEDMAR). Universidad Católica de Valencia. C/ Guillem de Castro, 94. 46003-Valencia. ana.m.blazquez@uv.es

[6] Instituto de Ciencia y Tecnología del Carbono (INCAR- CSIC), Francisco Pintado Fe 26, 33011-Oviedo. angeles.g.borrego@csic.es.

[7] Facultad de Ciencias. Universidad de Alcalá de Henares. 28805-Alcalá de Henares. blanca.ruiz@uah.es, mjose.gil@uah.es.

([*]) Corresponding author: joseeugenio.ortiz@upm.es

Abstract

We reconstructed the palaeoenvironmental conditions of Cartagena Bay during the Holocene after a multidisciplinary study to identify natural variations and the anthropic processes of this coastal area. A total of 119 samples were recovered for amino acid racemization dating, 3 for radiocarbon dating (^{14}C), and four sets of 80 samples for sedimentological and palaeontological determination, mineralogical content, biomarker and trace elements quantification. Two natural scenarios were identified from the variations of *n*-alkane indices and palaeobiological content. The first period (6,650–5,750 yr cal BP) was marked by the development of euhaline marine conditions with strong inputs from aquatic macrophytes and high biodiversity. After a hiatus, the area underwent a profound change, becoming a paucispecific brackish marsh environment with increasing inputs from land plants, with possible episodes of emersion with a greater presence from terrestrial gastropods (3,600–300 cal yr BP). By combining trace element abundance and stanol distributions, our study also provides a novel approach to identify the predominant influence of anthropogenic factors in the last three millennia in the coastal record of Cartagena Bay. Findings confirmed that Pb mining and metallurgy began during the Bronze Age, with considerable inputs of this heavy metal into the atmosphere during Phoenician, Punic and particularly Roman times compared to the Middle Ages. Pollution by Cu and Zn was also observed during Punic and Roman times, and was first documented in the Middle Ages. In addition, faecal stanols, such as coprostanol, derived mainly from humans, and 24-ethylcoprostanol from herbivores were present, thereby indicating for the first time a continuous presence of human populations and significant pollution input since 3,600 yr cal BP, this being greater in the late Bronze Age and Phoenician, Punic and Roman times than during Late Antiquity and the Middle Ages, when the city was in decline.

Key-words: ***n*-alkanes, faecal stanols, trace elements, palaeoenvironment, Southeastern Spain**

1. Introduction

Coastal marine areas are dynamic systems that hold valuable information about palaeoenvironmental conditions at a regional and global scale (Kraft et al., 1977; Pavlopoulos et al., 2006; Triantaphyllou et al., 2010; Torres et al., 2014). In addition, these areas are highly sensitive to direct pollution sources. Their sediments are therefore useful records of palaeoenvironmental change and human activity (Delile et al., 2014; Elmaleh et al., 2012; Le Roux et al., 2003, 2005; Stanley et al., 2007; Véron et al., 2006, 2013; Manteca et al., 2017). .

The ecosystems present in coastal environments are characterized by high biological productivity, due to the presence of a significant amount of organic matter (OM) from various sources affected by both marine and continental inputs (Hedges and Keil, 1995; González-Vila et al., 2003; Blázquez et al., 2018). In this regard, sedimentary biomarkers, such as aliphatic hydrocarbons (e.g., *n*-alkanes), are useful to study OM sources in coastal aquatic ecosystems and can contribute to environmental reconstructions (Volkman et al., 1980; 2008; Prahl and Carpenter, 1984; González-Vila et al., 2003; Blázquez et al., 2018).

Changes in lipid composition reflects environmental variations as, in most cases, OM is a mixture of components from multiple sources (algae, aquatic macrophytes, land plants) with variable degrees of preservation (Meyers, 2003). *n*-Alkanes are among the lipid biomarkers most commonly used as they are source-specific and have the advantage that they are less susceptible to microbial degradation than other compounds (Prahl and Carpenter, 1984; Meyers et al., 1995). In addition, the lipid compounds 5β-stanols are typically present in animal faeces, thus allowing the identification of faecal pollution (Leeming et al., 1984, 1996; Bethell et al., 1994; Shah et al., 2007) and allowing the identification of anthropic influence in sedimentary records.

Since prehistoric times, human activities have played an increasing role in the evolution of terrestrial and coastal ecosystems, generating impacts such as changes in the landscape and biotic communities, and atmospheric/water pollution. The anthropogenic signals of these activities are preserved in natural archives, such as coastal records, in the form of variations in the accumulation of chemical elements and compounds (Martínez Cortizas et al., 2005).

Metal mining and metallurgy have played a keys roles in world history, i.e., copper, lead and zinc have been progressively exploited mainly since the Chalcolithic (Killick and Fenn, 2012). In this regard, studies show that major atmospheric metal pollution started in the Bronze Age (Brännvall et al., 2001; Martínez Cortizas et al., 2002; Renberg et al., 2002; Monna et al., 2004; Kylander et al., 2005). The Iberian Peninsula has a long history of metal mining and metallurgy. Indeed, it was one of the main sources for metals in the Bronze Age (Leblanc et al., 2001; Hunt-Ortiz, 2003) and during the Roman Empire (Nriagu, 1983), the southeastern part of Spain, specifically around Cartagena (Murcia, SE Spain), being considered one of the areas where mining first took place. In this regard, this area has a rich ancient cultural heritage, as manifested by various archaeological sites containing relicts depicting the emergence and decline of highly populated and advanced societies.

To gain a full understanding of the environmental context affecting the choice of location for ancient cities in the Mediterranean realm and to capture environmental changes and their effect on societies, several studies have reconstructed the palaeoenvironment of their surroundings (Kraft et al., 1977, 2007; Pavlopoulos et al., 2006; Vött et al., 2006; Ghilardi et al., 2010; Triantaphyllou et al., 2010; Gébara and Morhange, 2010; Haenssler et al., 2013; Véron et al., 2013, 2018). However, scarce records covering the last 3000 yr are documented for the Iberian Peninsula.

Here the main goal was to gain new information to reconstruct the palaeoenvironmental evolution of the southeastern part of the Iberian Peninsula by interpreting the sedimentology, mineralogy, palaeontological content and biomarkers (*n*-alkanes) of sediments retrieved from Cartagena Bay. In addition, we also evaluated the influence and characteristics of anthropogenic activities using stanol content and trace elements for the first time.

It must be highlighted that SFT core contains a well-preserved and large record covering the last 3,600 yr (representing 7.5 m). Therefore, our study, which combines the measurement of trace elements of environmental concern (Pb, Zn and Cu), lipid distributions and palaeontological content in the coastal record of Cartagena Bay, provides a novel and detailed approach to improve the knowledge of the chemical imprints of natural processes and the growth of Cartagena, the most important city in the western Mediterranean realm since the Bronze Age, and nearby protohistorical and historical activities. Indeed, the largest Pb-Zn and Cu deposits of the western Mediterranean, which have been mined since ancient times, are located close to Cartagena.

2. Geographical and geological setting

The city of Cartagena is located on the southeastern tip of the Betic Cordillera, in the so-called Internal Zone. More precisely, it is situated on the boundary between two major geological and geomorphological units—to the south, the Sierra de Cartagena, a coastal mountain range, and to the north, the Neogene-Quaternary plain of the Campo de Cartagena, delimited by the Cartagena-La Unión fault (Fig. 1) (Manteca Martínez y García García 2004).

This region is characterised by the predominance of a warm and semi-arid ombro climate or arid warm Mediterranean climate: a subtropical steppe. The mean annual temperature is 20 °C and the annual rainfall is 270 mm (Rivas-Martínez and Rivas y Sáenz, 2017; Rodríguez Estrella et al., 2011).

Towards the north, there is El Almarjal, a marshy endorheic shallow depression 2 m above the local sea level, which had short phases of connection to the sea eastwards. It also received water and sediments from the Benipila, El Hondón and Saladillo Creeks. Its drainage basin extends over 72.5 km^2 (Conesa and García-García, 2003).

The bay opens from the mouth of the Benipila Creek—Mar de Mandarache—to the south. At its northern end, the bay lies on the hills of Cartagena, in which the remains of the ancient cities (Carthaginian and Roman) are found and which would have formed the "waterfront" during the Holocene. Mar de Mandarache, in the inner part of the estuarine environment, was a galley anchorage point, which was separated by a small sand bar of the wide marsh flat located to the north, El Almarjal.

3 Material and methods

A borehole with continuous core recovery was drilled in the Cartagena Basin, obtaining a 15 m deep core, named SFT. The core was inspected visually and the lithology, sedimentary structures, fauna content, and colour were noted.

Eighty samples were taken at regular intervals (ca. 10 cm) to study the sedimentology and fossil content, 3 samples were used for ^{14}C dating and 119 ostracode valves from 37 beds were analysed for amino acid racemisation dating. In addition, three sets of the same 80 samples were used for biomarker, X-ray diffraction and X-ray fluorescence analysis. The description of all methodologies are found in Suplementary Information.

4. Results

4.1 Chronological framework

The ages obtained by the radiocarbon method and AAR are shown in Tables 1 and 2 Supplementary information, respectively. The age of a single level was the average of the numerical ages obtained for Asx and Glx DL values (samples at 14.5 m and 14.3 m) or Asx DL values (rest of the levels) measured in the samples (Fig. 1 Supplementary information). Age uncertainty was the standard deviation of all the values obtained.

In general, the numerical datings obtained were consistent with depth, except the ^{14}C age of the sample at 9.6 m (1990±45 yr cal BP), which was much younger than the ages obtained using AAR for this bed and nearby ones (Table 2 Supplementary information). Moreover, the organic and inorganic geochemical data revealed marked differences below and above ca. 9.5 m, revealing a clear anthropic influence at < 9.5 m (sections 5.2 and 5.3) and suggesting an older age for this level. Therefore, we did not consider this ^{14}C age for the chronological model because of contamination and/or drilling operations.

The results revealed two markedly different age clusters: the lowermost part of the record (ca. > 14.2 m) was deposited during the Upper Pleistocene, whereas the upper 14.2 m belonged to the Holocene. Indeed, the lowest part of the record (15.0–14.2 m) comprised yellow sands, which were also observed in other cores of the area and were dated at the Upper Pleistocene (Torres et al., 2018).

Two chronological models were constructed for the Holocene record as a hiatus was observed: one model for the interval between 14.2 m and 9.5 (ca. 6,650 to 5,750 yr cal BP), and the other from 9.5 m to 3.0 m (< ca. 3,600 yr cal BP) (Fig. 1 Supplementary Information). These models were built using the Bayesian R-code package “Bacon 2.3.7” (Blaauw and Christen, 2011), both after 10,000 Markov Chain Monte Carlo iterations, as Bayesian age–depth modelling is considered more robust and flexible than other approaches.

4.2. Sedimentology and palaeontology

The SFT core (Fig. 2) was 15 m deep and consisted mainly of muds, sandy muds and fine-grain sands, in some cases with pottery sherds, especially at 9.0–8.5 m, 7.5–6.0 m, and 5.0–4.5 m, and a lead button at 3.8 m. Between 6.0 m and 4.8 m, breccias made of angular carbonate gravel were present. The upper part (< 1.6 m) of the core consisted of recent rubble and was not considered for the study. All beds showed reduced colours (grey to black), indicating the abundance of particulate OM. In some cases, minute charcoal fragments, showing their primary vegetal structure, were abundant. Plant seeds were also frequent.

Between 14.2 and 9.5 m, quartz was abundant, accounting for ca. 45% of the mineral content, followed by calcite (20%) and mica (20%). The upper 9.5 m showed clear mineralogical differences, as quartz decreased (ca. 30%), whereas calcite was predominant (40%), and dolomite was higher than in lower beds.

A total of 27 mollusc genera were identified (Fig. 2). In general, a high biodiversity of molluscs was observed between 14.2 and 9.5 m, dominated by *Hydrobia* sp., *P. conicus*, *Rissoa*, *Loripes*, *Cerastoderma*, *Retussa*, *Gastrana* and *Bivonia*. In contrast, in the uppermost 9.5 m, there was a sharp decrease in the diversity of mollusc genera, especially between 4.8 and 2.0 m, in which only *Hydrobia* was present, together with terrestrial gastropods. Between 6.0 and 4.8 m, fossils were virtually absent, coinciding with the breccia bed.

Cyprideis torosa was the predominant ostracode, forming monospecific accumulations in most cases (14.2–12.2 m, 9.5–6.0 m, 4.8–4.2 m), while at other levels *Loxoconcha* *elliptica*, *Loxoconcha rhomboidea* and *Aurila* sp. (12.2–9.5 m) and *Cypris* sp. (4.2–2.0 m) were also present. Miliolida were the most common foraminifers.

4.3 Biomarkers

4.3.1 n-Alkanes

Typical chromatograms of *n*-alkanes from selected samples are shown in Fig. 2 Supplementary Information. All the samples showed a predominance of odd carbon numbers, with a chain length distribution ranging mainly from C_{17} to C_{33}, maximising at C_{29} or C_{31}. The homologue C_{25} was predominant only in the lowermost part of the record.

The profiles of the various indices related to the *n*-alkane content, namely the predominant *n*-alkane chain length, the average chain length (ACL = (C_i x i + C_{i+1} x (i+1) + C_{i+2} x (i+2)...+ C_n x n))/ (Σ C_{n+1} + C_{n+2} + ...+ C_n), with i= 13, n = 33; Poynter, 1989)), the terrigenous/aquatic ratio of hydrocarbons (TAR_{HC} = (C_{31} + C_{29} + C_{27})/(C_{15} + C_{17} + C_{19}); Silliman et al., 1996), the aquatic macrophyte proxy (P_{aq} = (C_{23} + C_{25})/(C_{23} + C_{25} + C_{29} + C_{31}); Ficken et al., 2000), and the carbon preference index (CPI = ½ [(Σ C_i + C_{i+2} +...+ C_{i+8}) / (Σ C_{i-1} + C_{i+1} + ...+ C_{i+7}) + (Σ C_i + C_{i+2} +...+ C_{i+8}) / (Σ C_{i+1} + C_{i+3} + ...+ C_{i+9})], with i = 25 (Bray and Evans, 1961), are shown in Fig. 3.

The ACL index varied between 25.6 (9.9 m) and 30.0 (6.6 m), with a slightly increasing trend from the bottom to the top of the core. The lowest TAR_{HC} values (between 7.2 and 74.9) were found at the bottom (> 9.5 m), with a maximum values (> 100) in the uppermost 9.5 m. P_{aq} values ranged between 0.03 (6.6 m) and 0.42 (10.0 m) and showed a decreasing trend from the bottom to the top of the record. The CPI ratio showed oscillations, with values mainly > 8 in the upper 9.5 m of the record, with a maximum at 2.4 m (16.8), while values of between 3.1 and 7.3 were found in the lowermost 9.5 m.

4.4. Stanols

The main stanols identified in the core included 24-ethyl-5β-cholestan-3β-ol (24-ethylcoprostanol), 5β-cholestan-3β-ol (coprostanol), 5α-cholestan-3β-ol (cholestanol), 24-ethyl-5β-cholestan-3α-ol (24-ethylepicoprostanol) and 24-ethyl-5α-choles-22E-en-3β-ol (5α-stigmastanol).

It is worth noting that the uppermost 9.5 m of the core showed the highest stanol abundance (between 0.82 and 4.27 mg/kg), with a maximum at 8.5 m (10.48 mg/kg), whereas its concentration was very low below this depth (< 0.05 mg/kg) (Fig. 3). Also, between 6.0 and 4.8 m, the concentration of these compounds was low (0.04-0.82 mg/kg). The profiles of the various indices related to the stanol content used as proxies for distinguishing human vs. herbivore faecal input, namely the coprostanol/24-ethylcoprostanol ratio (Bethell et al., 1994; Evershed and Bethell, 1996) and the (coprostanol + epicoprostanol)/(24-ethylcoprostanol + 24-ethylepicoprostanol) ratio (Bull et al., 2002), are shown in Fig. 3. The values of these ratios were negligible below 9.5 m, peaked between 9.5 and 6.0 m (>1.0 and 1.5, respectively), and decreased in the uppermost 6.0 m (< 1.0).

4.5 Enrichment factors

Variations in the relative abundances of Pb, Zn and Cu through the core were studied to establish anthropogenic influence. To this end, the abundance of a given element was normalised to a conservative (lithogenic) element, calculating the [Me]/[X] ratio, where [Me] stands for the abundance of the element and [X] the abundance of the lithogenic element (a "conservative" element such as Ti, V or others).

Next, the [Me]/[X] ratio of the samples was normalised again to the [Me]/[X] ratio of samples from pre-anthropogenic times (Kylander et al., 2005; Mil-Homens et al., 2008). Here we normalised the abundances to Ti as other typical elements used for this purpose, such as V and Sc, were not analysed, and the abundance of Zr was low in most samples. The reference values for Me/Ti were taken from the baseline of the record, which is the average of samples below 10.5 m, which were clearly situated in pre-anthropogenic times. Thus, the enrichment factor (EF) of a certain element Me was calculated as:

$$MeEF_{Ti} = ([Me]/[Ti])_{sample}/([Me]/[Ti])_{reference}$$

To distinguish between anthropogenic vs. lithogenic inputs of Pb, Zn, and Cu, we followed the approach proposed by Shotyk et al. (2000). Thus, we calculated the abundance of lithogenic Pb, Zn and Cu as follows:

$$[Me]_{lithogenic}=[Ti]_{sample} \text{ x } ([Me]/[Ti])_{lithogenic}$$

where $[Me]_{lithogenic}$ is the abundance of Pb, Zn, and Cu. Once the lithogenic Pb, Zn and Cu components had been estimated, the anthropogenic concentration was easily calculated: $[Me]_{anthropogenic} = [Me]_{total} - [Me]_{lithogenic}$

Figure 4 shows the results obtained for the EF_{Ti} of Pb, Zn and Cu. To obtain a global vision of the accumulation of these elements, this information can be complemented with the concentration of lithogenic and anthropogenic Pb, Zn and Cu in the SFT core, calculated using Ti as a reference.

Of note, high abundances of lithogenic Pb (643-260), Zn (864-350) and Cu (158-64) were found in the lowermost part of the record (> 9.5 m) and they then decreased progressively. In contrast, anthropogenic values of Pb (45658-4374), Zn (2736-284) and Cu (1203-118) were markedly high in the upper 9.5 m, although the abundance of these metals decreased between 6.0 and 4.8 m, coinciding with the breccia bed.

5 Discussion

5.1. Palaeoenvironmental conditions

The CPI values observed in the core (> 4) indicated low degradation of *n*-alkanes and were thus interpreted in terms of the origin of OM input (cf. Hedges and Prahl, 1993; Zheng et al., 2007). The results indicated that the correlation coefficients between the CPI and the other indices (ACL, P_{aq}, TAR_{HC}) were significant (Table 1). The observed trend points to low microbial degradation of *n*-alkanes in these sediments and indicates the usefulness of *n*-alkane indices for interpreting palaeoenvironmental conditions in Cartagena.

There was generally good correspondence between the TAR_{HC} ratio, the predominant *n*-alkane chain and ACL values, a good proxy for distinguishing between low vs. high molecular weight *n*-alkanes (Pancost et al., 2002; Rommerskirschen et al., 2003) in the core, and an inverse correlation with the P_{aq} index (Table 1, Fig. 3). High TAR_{HC} values pointed to an increase in the input of terrestrial plants, whereas low values (< 1) were linked to a major input from algae (Silliman et al., 1996). It has to be considered that

TAR_{HC} may overestimate the contributions from terrestrial sources as terrestrial plants typically contain a greater proportion of *n*-alkanes than aquatic algae (Bourbonniere and Meyers, 1996). Furthermore, the lower molecular-weight *n*-alkanes (C_{15}, C_{17}, C_{19}) that typify algae are generally more susceptible to microbial degradation than land-plant n-alkanes (Meyers and Ishiwatari, 1993). This ratio nonetheless is valuable for determining changes in relative contributions of organic matter from land plants and algae (Bourbonniere and Meyers 1996). In this regard, the contrast between the low TAR_{HC} values in older sediments and the higher and more variable values since 3,600 yr cal BP (Fig. 3) reflected a change in geolipid sources. Thus, samples in which ACL and TAR_{HC} values were high coincided with low P_{aq} ratios.

The P_{aq} index was originally used to determine the relative contribution of aquatic macrophytes and terrestrial plants to some African lakes (Ficken et al., 2000), i.e., values < 0.1 are linked to a dominant contribution from land plants, typical in the upper 9.5 m, whereas those between 0.1 and 0.4, predominant below 9.5 m, reflect significant input from emergent macrophytes.

Thus, we interpret the significant inverse covariation between the P_{aq} index and TAR_{HC} values (a proxy for land plant contribution; r = –0.62) and ACL values (r = –0.89) as evidence of an episode marked by a major contribution from aquatic macrophytes (> 9.5 m), followed by a period in which the input from lands plants predominated.

5.2.1. Palaeoenvironmental scenarios

Using the predominant *n*-alkane chain, the ACL index, the P_{aq} values, the TAR_{HC} ratio, together with the mineralogical and fossil content, we defined two palaeoenvironmental scenarios in the Cartagena record.

Scenario A (14.2–9.5 m; (ca. 6,650–5,750 yr cal BP); Figs. 2, 3)**.** The predominant *n*-alkane corresponded to C_{29}, followed by C_{31}, indicating a major input from terrestrial plants. ACL values (average ca. 27.5) and the TAR_{HC} index (19-114) corroborated this interpretation, although P_{aq} (0.1–0.4) and CPI (ca. 4) values also indicated a significant input of aquatic macrophytes (Hedges and Prahl, 1993; Zheng et al., 2007; Ficken et al., 2000). These observations, together with the dominance of sandy muds and muddy sands, indicated low energy conditions and the development of a relatively flooded water mass with some marine influence (Ortiz et al., 2020). Quartz was abundant, accounting for ca. 45% of the total mineral content, and dolomite was present.

In addition, euhaline marsh conditions were interpreted by the presence of a rich biodiversity of ostracodes (*C. torosa*, *L. elliptica*, *L. rhomboidea*, *Aurila* sp.) and mollusc species (Richards, 1985; Torres et al., 2020) (Fig. 2).

Scenario B: This unit was identified between 9.5 m and 2.0 m (ca. 3,600–300 yr cal BP; Figs. 2, 3) above a hiatus. The predominant *n*-alkanes were C_{29} and C_{31}, which are linked to terrestrial plants. The high values of the ACL index (mostly between 28 and 30) and TAR_{HC} (> 100) and the markedly low P_{aq} index (< 0.1) confirmed this interpretation, with a decreasing input of aquatic macrophytes and algae with respect to land plants. Higher CPI values in this unit than in the others (> 8) confirmed that input of terrigenous plants was more significant (Hedges and Prahl, 1993; Zheng et al., 2007).

Consistent with this interpretation, there was a predominance of grey/dark muds and sandy muds, which points to a lower input from runoff and low energy conditions.

In this regard, a notable presence of calcite (> 40%) and a decrease in quartz confirmed low energy conditions. There was a limited presence of mollusc remains, thereby indicating a shallow, brackish, paucispecific distribution of species, dominated by *Hydrobia* sp., *Cerithium* sp., and *P. conicus* (Rohde and Sandland, 1975; Richards, 1985). Moreover, ostracodes were represented by the monospecific presence of *C. torosa*, which was sometimes accompanied by *Cypris* sp between 4.2 and 2.0 m. The occurrence of this ostracode and mollusc association reveals the development of a brackish marshland with some freshwater influence at the top.

It must be highlighted that between 6.0 and 4.8 m, a gravel bed made of angular calcareous clasts occurred, linked to flash flood episode, probably associated with the activity of the Benipila creek, whose catchment area lies on Mesozoic limestones. Nevertheless, this bed also contained civil work-debris of the ancient city. This high-flow would have diluted the concentration of trace elements and stanols (Figs. 3, 4), although, in our view, human activity (metallurgy, farming and waste) did not significantly change.

5.2 Organic pollution

5β-Stanols are commonly formed as reduction products of cholesterol and the higher molecular weight counterparts (campesterol, sitosterol and stigmasterol) in the intestinal tracts of most mammals (Bull et al., 2002), and they can accumulate in sediments. Cholesterol is converted to 5β-coprostanol in the human digestive tract (Murtaugh and Bunch, 1967; Leeming et al., 1984; Bethell et al., 1994; Shah et al., 2007). However, this compound is relatively less abundant in the faeces of other animals (Leeming et al. 1996; Mudge and Morrison, 2010). In contrast, herbivores tend to produce 24-ethylcoprostanol from β-sitosterol (abundant in plants). Thus, stanol content, specifically the type of coprostanol, can be used to distinguish human input from that of herbivores (Leeming and Nichols, 1996; Leeming et al., 1996).

We interpreted the organic pollutant history from the 5β-stanol content in the SFT core in the context of the occupation of Cartagena by human populations. The concentrations of these compounds were markedly low below 9.5 m (> 5,750 yr cal BP), when Cartagena had still not been founded. In contrast, we observed a continuous presence of 5β-stanols in the uppermost 9.5 m of the core, which corresponded to the last ca. 3,600 yr cal BP, thus corroborating the presence of humans and cattle since the late Bronze Age. Among these compounds, it is worth noting the presence of 24-ethylcoprostanol and coprostanol, considered biomarkers of herbivore and human faecal pollution, respectively.

Bethell et al. (1994) and Evershed and Bethell (1996) proposed the use of the coprostanol/24-ethylcoprostanol ratio as a proxy for distinguishing human vs. herbivore faecal input, with values > 1.5 considered indicative of human pollution and < 0.25 predominance of herbivore faeces. An extension of this approach to estimate the relative contribution of different faecal sources was proposed by Bull et al. (2002) (coprostanol + epicoprostanol)/(24-ethylcoprostanol + 24-ethylepicoprostanol) to distinguish between contamination by humans (> 1) and ruminant species (< 1).

Between 9.5 and 6.0 m of the SFT core (3,600–1,700 yr cal BP, Fig. 3), the values of this ratio were > 1, indicating a continuous source of organic pollution derived mainly from humans and thus pointing to a large population in the ancient city of Cartagena. In contrast, in the uppermost levels (6.0–2.0 m) of the core (last 1,700 yr), the concentration of 24-ethylcoprostanol was markedly higher than in the rest of the record (Fig. 3). This finding is attributed to cattle faeces reaching the water body through surface runoff, linked to a decrease in population.

We confirmed the major influence of human faeces between 3,600 and 1,700 yr cal BP on the basis of the values of the coprostanol/24-ethylcoprostanol ratio (> 1.5). However, we can establish that, at younger ages, there was a mixture of organic pollutants from humans and herbivores, the latter being slightly more predominant.

5.3 Metal pollution

5.4.1 Pb

In the lower part of the record (> 9.5 m, > 5,750 yr cal BP - Fig. 5), $PbEF_{Ti}$ values were low, indicating no considerable input of Pb to Cartagena Bay, which was mostly of lithogenic origin. However, in the uppermost part of the record, the values increased significantly, especially between 9.5 and 6.2 m. Thus, in the last 3,600 yr cal. BP, we interpreted that the evolution of the $PbEF_{Ti}$ was mostly linked to atmospheric pollution caused by mining and metallurgical processes in the late Bronze Age and during Phoenician, Punic and Roman times, the Middle Ages and the Modern Age rather than to natural variations or sedimentological characteristics.

Of note, the maximum input of anthropogenic Pb occurred during Roman times. These results are in coincidence with those of Manteca et al. (2017) and Ortiz et al. (2021), who observed that atmospheric Pb pollution began ca. 4,250 years ago, with high values during Phoenician, Punic and Roman times. This pattern has also been observed in other regions of Spain (Martínez Cortizas et al., 1997, 1999, 2002a; Fábregas et al., 2003; Gallego et al., 2013, 2019) and Europe (Weiss et al., 1997; Shotyk et al., 2001).

Indeed, it is estimated that 60% of ancient Pb production in Spain occurred during Roman times (Nriagu, 1983). A similar enrichment of Pb was found for the Roman age in Germany, Norway, Belgium, Scotland, Sweeden and Switzerland (Kempter et al., 1997; Weiss et al., 1997; Shotyk et al., 2001; Renberg et al., 2002).

Anthropogenic Pb decreased significantly after the end of the Roman Empire until the beginning of Late Antiquity, a finding also reflected in other proxies, coinciding with the gravel bed (breccia) linked to a flash flood episode. This decrease could be also attributable to the final years of the Roman Empire and the decline of mining and metallurgy in Cartagena. The concentration of Pb increased from ca. 1,400 yr cal BP but never recovered previous values.

5.4.2 Zn

Natural inputs of Zn were greater than those of anthropogenic sources, although Zn from the latter increased in the uppermost part of the record (ca. 3,000 yr cal BP), reaching two maxima: during the Phoenician period (ca. 2,800 yr cal BP) and during Punic and Roman times (2,300–2,000 yr cal BP). This observation brings forward the age of Zn presence in the area of Cartagena, as Manteca et al. (2017) and Ortiz et al. (2021) observed an increase in Zn content only in Roman times, with a maximum at ca. 1,700 yr cal BP. Indeed, on the basis of the first evidence of atmospheric Zn pollution recorded in northern Spain, Martínez Cortizas et al. (1997) proposed that it began at ca. 1,000 AD, associated with the metallurgy of other metal ores. Anthropogenic Zn decreased between 1,700 and 1,400 yr cal BP coinciding with the gravel bed and then recovered previous values.

The Zn profiles did not show a clear relationship with those of Pb. This finding was also reported in other records (Martínez-Cortizas et al., 1997; Gallego et al., 2013, 2019). Of note, Zn values were higher than those of Pb before 3,600 yr cal BP. This behaviour is explained by the metal contribution to the basin coming only from natural origins, at least before 3600 yr cal BP. Indeed, Zn content has greater abundance in the source area than Pb (Manteca y Ovejero, 1992).

In contrast, starting on that date, the Pb content significantly surpassed that of Zn due to the development of an early mining and metallurgical industry based on Pb ores, with Zn playing only an accessory role (Manteca et al., 2017). However, at ca. 900 yr cal BP, there was a peak in the Zn abundance, which might be attributable to the mining of a certain ore (Ag) containing this metal. In this regard, Ag (and Pb) mining activities near Cartagena were significant during the early Middle Ages, with Zn (sphalerite) usually associated with these ores.

5.4.3 Cu

It is worth noting that Pb and Cu signals were not coincident, thereby suggesting that they may have derived from different mines or that the Romans turned their interest away from Pb to Cu. However, a technological change cannot be discarded.

The Cu profile showed an increase coinciding with the Phoenician period (ca. 2,800 yr cal BP) and the Punic and Roman times (4.5 m, 2,300–2,000 yr cal BP, Fig. 5). This increase was linked mainly to anthropogenic sources, indicating a major input derived from mining activities in this area, consistent with observations made by Hong et al. (1996), who reported a sharp rise of world Cu production at ca. 2,500 yr cal BP. Indeed, during Roman times, the main Cu mining regions were in Spain, which accounted for more than half the worldwide production of this metal (Darling, 1990). In this regard, the Punics and Romans appear to have worked Ag deposits, which are linked to those of Cu (Darling, 1990). In fact, in the Phoenician site of La Fonteta (Guardamar del Segura, Alicante), close to Cartagena, materials used in Pb and Ag production, as well as in Cu-based metallurgy, were found, and cuproargentiferous ores were probably exploited (Renzi et al., 2009). Of note, those authors reported that anthropogenic Cu input peaked in the early Middle Ages. Indeed, a peak in anthropogenic Cu was observed at ca. 1300-1200 yr cal BP. Thus, Cu abundance could be explained by the metallurgy of Ag sulphides. In this regard, numerous kilns that were active during the Middle Ages have been documented in Cartagena mountains (Grañeda, 2008). Nevertheless, this increase in Cu abundance could be also associated with the important exploitation of alum deposits in the area of Cartagena during the Middle Ages, as such deposits are commonly linked to Cu sulphate minerals (Pérez Macías, 2019).

6 Conclusions

The use of amino acid racemization and ^{14}C dating allowed us to establish the chronological framework of the palaeoenvironmental evolution of the Cartagena Bay during the Holocene and the anthropic processes that affected this coastal area.

A novel multidisciplinary study combining sedimentology, palaeontology, and mineralogical and biomarker content allowed us to distinguish two main palaeoenvironmental scenarios in the Holocene record: 1) between ca. 6,650 and 5,750 yr cal BP, the main input of OM came from aquatic macrophytes and algae in a euhaline coastal area with high biodiversity, and 2) between ca. 3,600 and 300 yr cal BP, the main input was from land plants, thereby indicating a shallower water body (marsh), with brackish conditions, as reflected by the paucispecific fauna, with low energy conditions, although flash flood episodes occurred. At the top of the record, freshwater inputs may have occurred, together with some episodes of emersion.

Our study also revealed that the influence of anthropogenic inputs was considerable in the last three millennia, i.e., faecal stanols and trace elements were used together for the first time to reconstruct the emergence (3,600–1,700 yr cal BP) and decline (< 1,700 yr) of the ancient city of Cartagena, the most important settlement in southwestern Mediterranean since the Bronze Age. In this regard, it is worth noting that scarce records covering the last 3000 yr are documented for the Iberian Peninsula. Pb exploitation and metallurgy occurred since, at least, the Bronze Age, with a significant increase during Phoenician, Punic and particularly Roman times. In contrast, Pb pollution during the Middle Ages decreased. The Cu and Zn signals derived from anthropogenic sources were also significant during Phoenician and Punic times, reaching maximum values during Roman times. Moreover, there was a considerable input of these elements in the Middle Ages, which was not previously documented.

Acknowledgments

This paper was made possible by Grant HAR2017-85726-C2-2-P (*Cambios ambientales y ocupación humana en el sector central del sureste ibérico*) funded by MCIN/AEI/

10.13039/501100011033 and by Grant HAR2017-85726-C2-1-P (*Carthago Nova desde su entorno litoral: Paleotopografía y evolución medioambiental del Sector central del Sureste Ibérico. Dinámica poblacional y productiva*) funded by MCIN/AEI/ 10.13039/501100011033.. XRF core scanner equipment was co-financed by the European Regional Development Fund via the Spanish National Plan for Scientific and Technical Research and Innovation 2013-2016 (IGME13-4E-2576).

References

Arduino, G., Arduino, M., Nappo, A., Nappo, S., 2016. Conchiglie del Mediterraneo. Available at: http://www.conchigliedelmediterraneo.it/ (accessed 10 January 2021).

Bethell, P.H., Goad, L.J., Evershed, R.P., Ottaway, J., 1994. The study of molecular markers of human activity: the use of coprostanol in the soil as an indicator of human faecal material. J Archaeol. Sci. 21, 619–632. https://doi.org/10.1006/jasc.1994.1061

Blaauw, M., Christen, J.A., 2011. Flexible paleoclimate age-depth models using an autoregressive gamma process. Bayesian Anal. 6, 457-474. https://doi.org/10.1214/11-BA618

Blázquez et al., 2018, Rodríguez-Pérez, A., Torres, T., Ortiz, J.E., 2017. Evidence for Holocene sea level and climate change from Almenara marsh (western Mediterranean). Quat. Res. 88, 206-222. https:// DOI:10.1017/qua.2017.47

Bode, M., Rothenhoefer, P., Hanel, N., Hauptmann, A., 2015. Lead-silver mines of the Iberian Peninsula and their exploiters: a reconstruction of roman lead production in southeastern Spain. Abstract book of the 4th Archaeometallurgy in Europe International Conference (Madrid, 1st-3rd June, 2015), 80 pp.

Bourbonniere, R.A., Meyers, P.A., 1996. Anthropogenic influences on hydrocarbon contents of sediments deposited in eastern Lake Ontario since 1800. Environ. Geol. 28, 22-28. https://doi.org/10.1007/s002540050074

Brännvall, M.-L., Bindler, R., Emteryd, O., Renberg, I., 2001. Vertical distribution of atmospheric pollution lead in Swedish boreal forest soils. Water Air Soil Pollut. 1, 357–376. https://doi.org/10.1023/A:1017513802959

Bray, E.E., Evans, E.D., 1961. Distribution of n-paraffins as a due to recognition of source beds. Geochim. Cosmochim. Acta 22, 2–15. https://doi.org/10.1016/0016-7037(61)90069-2

Bright, J., Kaufman, D. S., 2011. Amino acid racemization in lacustrine ostracodes, part I: effect of oxidizing pre-treatments on amino acid composition. Quat. Geochron. 6, 154-173. https://doi.org/10.1016/j.quageo.2010.11.006

Bull, I.D., Lockheart, M.J., Elhmmali, M.M., Roberts, D.J., Evershed, R.P., 2002. The origin of faeces by means of biomarker detection, Environmental International 27, 647–654. https://doi.org/10.1016/S0160-4120(01)00124-6

Carbonel, P., 1985. Néogène, in: Oertli, H.J. (ed), Atlas des ostracodes de France. Bull. Centr. Rech. Explor.-Prod. Elf-Aquitaine 9, 311-335.

Conesa, C., García-García, E., 2003. Las áreas históricas de inundación en Cartagena: problemas de drenaje y actuaciones. B. Asoc. Geogr. Esp. 35, 79-100.

Darling, A.S., 1990. Non ferrous metals in: McNeil, B. (Ed.), An Encyclopaedia of the History of Technology. Routledge, London, pp. 47-145.

Delile, H., Mazzini, I., Blichert-Toft, J., Goiran, J.P., Arnaud-Godet, F., Salomon, F., Albarede, F., 2014. Geochemical investigation of a sediment core from the Trajan basin at Portus, the harbor of ancient Rome. Quat. Sci. Rev. 87, 34–45. https://doi.org/10.1016/j.quascirev.2014.01.002

Domergue, C., 1987. Catalogue des mines et fonderies antiques de la Peninsule Ibérique. Publication de la Casa de Velazquez, Serie Archeologie VIII, Madrid.

Domergue, C., 1990. Les mines de la Peninsule Ibérique dans l'Antiquité romaine. Publications de l'École Française de Rome 127, 1-696.

Elmaleh, A., Galy, A., Allard, T., Dairon, R., Day, J.A., Michel, F., Marriner, N., Morhange, C., Couffignal, F., 2012. Anthropogenic accumulation of metals and metalloids in carbonate-rich sediments: insights from the ancient harbor setting of Tyre (Lebanon). Geochim. Cosmochim. Acta 82, 23–38. https://doi.org/10.1016/j.gca.2011.04.032

Evershed, R.P., Bethell, P.H., 1996. Application of multimolecular biomarker techniques to the identification of fecal material in archaeological soils and sediments. Archaeol. Chem. 625, 157-172. https//10.1021/bk-1996-0625.ch013

Fábregas Valcarce, R., Martínez Cortizas, A., Blanco Chao, R., Chesworthd, W., 2003. Environmental change and social dynamics in the second–third millennium BC in NW Iberia. J. Archaeol. Sci. 30, 859-871. https://doi.org/10.1016/S0305-4403(02)00264-9

Ficken K.J., Li, B., Swain, D. L. Eglinton G., 2000. An n-alkane proxy for the sedimentary input of submerged/floating freshwater aquatic macrophytes. Org. Geochem. 31, 745–749. https://doi.org/10.1016/S0146-6380(00)00081-4

Gallego, J.L.R., Ortiz, J.E., Sierra, C., Torres, T., Llamas, J.F., 2013. Multivariate study of trace element distribution in the geological record of Roñanzas Peat Bog (Asturias, N. Spain). Paleoenvironmental evolution and human activities over the last 8000 cal yr BP. Sci. Total Environ. 454-455, 16-29. https://doi.org/10.1016/j.scitotenv.2013.02.083

Gallego, J.L.R., Ortiz, J.E., Sánchez-Palencia, Y., Baragaño, D., Borrego, A., Torres, T., 2019. A multivariate examination of the timing and accumulation of potentially toxic elements at Las Conchas bog (NW Spain). Environ. Poll. 254, 1-13. https://doi.org/10.1016/j.envpol.2019.113048

Gardner Moore, F., 1970. Livius, T., The History of Rome in Fourteen Volumes, vol. VII, Books XXVI-XXVII (English translation), The Loeb Classical Library, London.

Gébara, C., Morhange, C., 2010. Fréjus (Forum Iulii): le port antique/The ancient harbour. J. Roman Archaeol. 152 Suppl. Series 77, 152 pp. https://doi.org/10.3764/ajaonline1154.Moore

Ghilardi, M., Genç, A., Syrides, G., Bloemendal, J., Psomiadis, D., Paraschou, T., Kunesch, S., Fouache, E., 2010. Reconstruction of the landscape history around the remnant arch of the Klidhi Roman Bridge, Thessaloniki Plain, North Central Greece. J. Archaeol. Sci. 37, 178–191. https://doi.org/10.1016/j.jas.2009.09.030

Gofas, S., Salas, C., Moreno, D., 2011. Moluscos marinos de Andalucía (vol 1). Málaga: *Servicio de Publicaciones e Intercambio Científico, Universidad de Málaga*

González-Vila, F.J., Polvillo, O., Boski, T., Moura, D., de Andrés, J.R., 2003. Biomarker patterns in a time-resolved Holocene/terminal Pleistocene sedimentary sequence from the Guadiana river estuarine area (SW Portugal/Spain border). Org. Geochem. 34, 1601–1613. https://doi.org/10.1016/j.orggeochem.2003.08.006

Grañeda, P., 2008. La explotación andalusí de los metales preciosos: los trabajos a bocamina. Boletín del Museo Arqueológico Nacional 24-25-26, 141-154.

Guillaume M.C., Peypouquet, J.P., Tetart, J., 1985. Quaternaire et Actuel. In: Oertli, H.J. (Ed.), Atlas des ostracodes de France. Bull. Cent. Rech. Explor. Prod. Elf-Aquitaine 9, 337-377.

Haenssler, E., Nadeau, M.J., Vott, A., Unkel, I., 2013. Natural and human induced environmental changes preserved in a Holocene sediment sequence from the Etoliko Lagoon, Greece: new evidence from geochemical proxies. Quat. Int. 308–309, 89–104. https://doi.org/10.1016/j.quaint.2012.06.031

Hearty, P.J., O'Leary, M.J., Kaufman, D.S., Page, M., Bright, J., 2004. Amino acid geochronology of individual foraminifer (*Pulleniatina obliquiloculata*) tests, north Queensland margin, Australia: a new approach to correlating and dating Quaternary tropical marine sediment cores. Paleoceanography 19, PA4022. https://doi: 10.1029/2004PA001059.

Hedges, J.I., Keil, R.G., 1995. Sedimentary organic matter preservation: an assessment and speculative synthesis. Mar. Chem. 49, 81–115. https://doi.org/10.1016/0304-4203(95)00008-F

Hedges, J.I., Prahl, F.G., 1993. Early diagenesis: consequences for applications of molecular biomarkers, in: Engel, M.H., Macko, S.A. (Eds.), Organic Geochemistry. Principles and Applications. Plenum Press, New York. pp. 237-253.

Hunt-Ortiz, M.A., 2003. Prehistoric mining and metallurgy in south-west Iberian Peninsula. BAR International Series 1188. Archaeopress, Oxford.

Kempter, H., Görres, M., Frenzel, B., 1997. Ti and Pb concentrations in rainwater-fed bogs in Europe as indicators of past anthropogenic activities. Water Air Soil Pollut. 100, 367-377. https://doi.org/10.1023/A:1018376509985

Kaufman, D.S., 2000. Amino acid racemization in ostracodes, in: Goodfriend, G.A., Collins, M.J., Fogel, M.L., Macko, S.A., Wehmiller, J.F. (Eds.), Perspectives in Amino Acids and Protein Geochemistry. Oxford University Press, New York, pp. 145-160.

Kaufman, D.S., Manley, W.F., 1998. A new procedure for determining DL amino acid ratios in fossils using reverse phase liquid chromatography. Quat. Geochron. 17, 987-1000. https://doi.org/10.1016/S0277-3791(97)00086-3

Killick, D., Fenn, T., 2012. Archaeometallurgy: the study of preindustrial mining and metallurgy. Annu. Rev. Anthropol. 41, 559–575. https:// doi:10.1146/annurev-anthro-092611-145719

Kraft, J. C., Brückner, H., Kayan, I., Engelmann, H., 2007. The 1579 geographies of ancient Ephesus and the Artemision in Anatolia. Geoarchaeology 22, 121–149. https://doi.org/10.1002/gea.20151

Kraft, J.C., Aschenbrenner, S.E., Rapp Jr., G., 1977. Palaeogeographic reconstructions of coastal Aegean archaeological sites. Science 195, 941–947. https://doi.org/10.1126/science.195.4282.941

Kylander, M.E., Weiss, D.J., Martínez Cortizas, A., Spiro, B., García-Sánchez, R., Coles, B.J., 2005. Refining the pre-industrial atmospheric Pb isotope evolution curve in Europe using an 8000 year old peat core from NW Spain. Earth Planet. Sci. Lett. 240, 467-485. https://doi.org/10.1016/j.epsl.2005.09.024

Le Roux, G., Morhange, C., Véron, A., 2005. Lead pollution in the ancient harbor of Marseilles. Méditerranée 1, 31–35.

Le Roux, G., Veron, A., Morhange, C., 2003. Geochemical evidences of early anthropogenic activity in harbour sediments from Sidon. Archeol. Hist. Leb. 18, 115–119.

Leeming, R., Ball, A., Ashbold, G.N., Jones, P. Nichols, J.P., 1984. Distinguishing between human and animal sources of fecal pollution. Aus. J. Chem. 61, 434–435. https://doi.org/10.1504/IJW.2009.023080

Leeming, R., Ball, A., Ashbolt, N., Nichols, P., 1996. Using faecal sterols from humans and animals to distinguish faecal pollution in receiving waters. Water Res. 30, 2893-2900. https://doi.org/10.1016/S0043-1354(96)00011-5

Leeming, R., Latham, V., Rayner, M., Nichols, P., 1997. Detecting and distinguishing sources of sewage pollution in Australian inland and coastal waters and sediments, in: Eganhouse, R.P. (Ed.), Application of Molecular Markers in Environmental Geochemistry. American Chemical Society National Meeting, Orlando, ACS Washington, DC, pp. 306-319

Leeming, R., P. Nichols. 1996. Concentrations of coprostanol that correspond to existing bacterial indicator guideline limits. Water Res. 30, 2997-3006. https://doi.org/10.1016/S0043-1354(96)00212-6

Manteca Martínez, J.I.,, García García, C., 2004. La falla de Cartagena-La Unión. Aportación a su conocimiento y verificación visual de su existencia gracias a una obra pública. Actas V Reunión Comisión Patrimonio Geológico de la Sociedad Geológica de España, pp: 239–246.

Manteca, J.I., Ovejero, G., 1992. Los yacimientos Zn, Pb, Ag-Fe del distrito minero de La Unión-Cartagena, Bética Oriental. In: García Guinea, J., Martínez Frías, J. (eds.), Recursos Minerales de España. CSIC, Madrid, pp. 1085-1102.

Manteca, J.I., Ros, M., Ramallo, S., Navarro, F., Rodríguez-Estrella, T., Cerezo, F., Ortiz, J.E., Torres, T., 2017. Early metal pollution in Southwestern Europe: the former littoral lagoon of el Almarjal (Cartagena mining district S.E. Spain) A sedimentary archive more than 8000 years old. Env. Sci. Pollut. 24, 10584-10603. https://doi.org/10.1007/s11356-017-8682-5

Martínez Cortizas, A., García-Rodeja, E., Pontevedra Pombal, X., Nóvoa Muñoz, J.C., Weiss, D., Cheburkin, A., 2002. Atmospheric Pb deposition in Spain during the last 4600 years recorded by two ombrotrophic peat bogs and implications for the use of peat as archive. Sci. Total Environ. 292, 33–44. https://doi.org/10.1016/S0048-9697(02)00031-1

Martínez Cortizas, A., Mighall, T., Pontevedra Pombal, X., Novoa Muño, J.C., Peiteado Varela, E., Piñeiro Rebolo, R., 2005. Linking changes in atmospheric dust deposition, vegetation change and human activities in northwest Spain during the last 5300 years. The Holocene 15, 698-706. https://doi.org/10.1191/0959683605hl834rp

Martínez Cortizas, A., Pontevedra Pombal, X., Nóvoa Muñoz, J.C., García-Rodeja, E., 1997. Four thousand years of atmospheric Pb, Cd and Zn deposition recorded by the ombrotrophic peat bog of Penido Vello (northwerstern Spain). Water Air Soil Pollut. 100, 387-403. https://doi.org/10.1023/A:1018312223189

Martínez Cortizas, A., Pontevedra-Pombal, X., García-Rodeja, E., Nóvoa-Muñoz, J.C., Shotyk, W., 1999. Mercury in a Spanish Peat Bog: Archive of Climate Change and Atmospheric Metal Deposition. Science 284, 939-942. https://doi.org/10.1126/science.284.5416.939

Martínez-García, B., Pascual, A., Rodríguez-Lázaro, J., Martín-Rubio, M., Rofes, J., 2013. The Ostracoda (Crustacea) of the Tina Menor estuary (Cantabria, southern Bay of Biscay): Distribution and ecology. J. Sea Res. 83, 111-122. https://doi.org/10.1016/j.seares.2013.03.014

Mazzini, I., Anadón, P., Barbieri, M., Castorina, F., Ferreli, L., Gliozzi, E., Mola, M., Vittori, E., 1999. Late Quaternary sea-level changes along the Tyrrhenian coast near Orbetello (Tuscany, central Italy): palaeoenvironmental reconstruction using ostracods. Mar. Micropaleontol. 37, 289-311. https://doi.org/10.1016/S0377-8398(99)00023-7

Meana, M.J., Piñero, F., 1998. Strabo, P., Geografía, volume II: books III-IV (Spanish translation). Editorial Gredos, Madrid.

Meyers, P.A., 2003. Applications of organic geochemistry to paleolimnological reconstructions: a summary of examples from the Laurentian Great Lakes. Org. Geochem. 34, 261-289. https://doi.org/10.1016/S0146-6380(02)00168-7.

Meyers, P.A., Leenheer, M.J., Eaoie, B.J., Maule, S.J., 1984. Organic geochemistry of suspended and settling particulate matter in Lake Michigan. Geochim. Cosmochim. Acta 48, 443-452. https://doi.org/10.1016/0016-7037(84)90273-4

Meyers, P.A., Leenheer, M.J., Bourbonniere, R.A., 1995. Diagenesis of vascular plant organic matter components during burial in lake sediments. Aquat. Geochem 1, 35-42. https://doi.org/10.1007/BF01025230

Meyers, P.A., Ishiwatari, R., 1993. Lacustrine organic geochemistry-an overview of indicators of organic matter sources and diagenesis in lake sediments. Org. Geochem. 20, 867-900. https://doi.org/10.1016/0146-6380(93)90100-P

Mil-Homens, M., Branco, V., Vale, C., Stevens, R., Boer, W., Lebreiro, S., Cato, I., Abrantes, F., 2008. Historical trends in Hg, Pb and Zn sedimentation in the central shelf area of Portugal. J. Iber. Geol. 34, 287-298.

Monna, F., Galop, D., Carozza, L., Tual, M., Beyrie, A., Marembert, F., Chateau, C., Dominik, J., Grousset, F.E., 2004. Environmental impact of early Basque mining and smelting recorded in a high ash minerogenic peat deposit. Sci. Total Environ. 32, 197–214. https://doi.org/10.1016/j.scitotenv.2004.01.010

Mudge, S., Morrison, A.M., 2010. Tracking sources of sewage in the environment. Environmental Notes 9, 1-4.

Murtaugh, J.J., Bunch, R.L., 1967. Sterols as a measure of fecal pollution. J. Water Pollut. Control Fed. 39, 404-409. http://www.jstor.org/stable/25035758.

Nachite, D., Rodríguez-Lázaro, J., Martín-Rubio, M., Pascual, A., Bekkali, R., 2010. Distribution et écologie des associations d'ostracodes récents de l'estuaire de Tahadart (Maroc Nord-Occidental). Rev. de Micropaléontol. 53, 3-15. https://doi.org/10.1016/j.revmic.2008.04.004

Nriagu, J.O., 1983. Lead and Lead Poisoning in the Antiquity. Wiley, New York.

Ortiz, J.E., Torres, T., Julià, R., Delgado, A., Llamas, F.J., Soler, V., Delgado, J., 2004. Numerical dating algorithms of amino acid racemization ratios from continental ostracodes. Application to Guadix-Baza basin (southern Spain). Quat. Sci. Rev. 23, 717-730. https://doi.org/10.1016/j.quascirev.2003.06.001

Ortiz, J.E., Torres, T., Pérez González, A., 2013. Amino acid racemization in four species of ostracodes: taxonomic, environmental, and microstructural controls. Quat. Geochron. 16, 129-143. https://doi.org/10.1016/j.quageo.2012.11.004

Ortiz, J.E., Torres, T., Ramallo, S.F., Ros, M., 2015. Algoritmos de datación por racemización de aminoácidos de ostrácodos del Holoceno y Pleistoceno superior en la Península Ibérica. Geogaceta 58, 63-66.

Ortiz, J.E., Torres, T., Sánchez-Palencia, Y., Ros, M., Navarro, F., López-Cilla, I., Galán, L.A., Ramallo, S., Rodríguez-Estrella, T., Blázquez, A., 2020. Biomarkers in coastal marshlands: environmental characteristics of the Mazarrón Basin during the Middle Pleistocene (MIS 7) and Holocene (MIS 1). Org. Geochem. 149, https://doi.org/10.1016/j.orggeochem.2020.104117

Ortiz, J.E., Torres, T., López-Cilla, I., Galán, L.A., Sánchez-Palencia, Y., Ros, M., Manteca, I., Ramallo, S., Navarro, F., Rodríguez-Estrella, T., Blázquez, A., Gómez-Borrego, A., Ruiz-Zapata, B., Gil, M.J., Heine, E., 2021. Keys to discern the Phoenician, Punic and Roman mining in a typical coastal environment through the multivariate study of trace element distribution. Sci. Total Env. 790, https://doi.org/10.1016/j.scitotenv.2021.147986.

Palahi, T., 2016. Apianus, Historia de Roma sobre Iberia (Spanish translation). Luarna Ediciones, Madrid.

Pancost, R.D., Baas, M., van Geel, B., Sinninghe Damsté, J.S., 2002. Biomarkers as proxies for plant inputs to peats: an example from a sub-boreal ombotrophic bog. Org. Geochem. 33, 675-690. https://doi.org/10.1016/S0146-6380(02)00048-7

Paton, W.R., 1968. Polybius, The Histories (English translation), William Heinemann Ltd, London.

Pavlopoulos, K., Karkanas, P., Triantaphyllou, M., Karymbalis, E., Tsourou, T., Palyvos, K., 2006. Paleoenvironmental evolution of the coastal plain of Marathon, Greece, during the Late Holocene: depositional environment, climate, and sea level changes. J. Coast. Res. 22, 424–438. https://doi.org/10.2112/03-0145.1

Pérez Macías, J.A., 2019. La minería metálica en Al-Andalus. In: Delgado Pérez, M.C., Pérez-Aguilar, L.G. (eds.), Economía y trabajo: Las bases materiales de la vida en Al-Andalus. Ediciones Alfar, Sevilla, pp. 237-253.

Poynter, J.G., 1989. Molecular stratigraphy: The Recognition of Palaeoclimatic Signals in Organic Geochemical Data. PhD Thesis, University of Bristol.

Prahl, F.G., Carpenter, R., 1984. Hydrocarbons in Washington coastal sediments. Estuar. Coast. Shelf Sci. 18, 703-720. https:// doi:10.1016/0272-7714(84)90040-4

Ramallo, S.F., Berrocal, M.C., 1994. Mineria púnica y romana en el sureste peninsular: el foco de Carthago Nova, in: Vaquerizo, D. (Ed.), Minería y metalurgia en la España prerromana y romana. Área de Cultura de la Excelentísima Diputación Provincial de Córdoba, pp. 79–146.

Reimer, P., Austin, W.E.N., Bard, E., Bayliss, A., Blackwell, P.G., Bronk Ramsey, C., Butzin, M., Cheng, H., Edwards, R.L., Friedrich, M., Grootes, P.M., Guilderson, T.P., Hajdas, I., Heaton, T.J., Hogg, A.G., Hughen, K.A., Kromer, B., Manning, S.W., Muscheler, R., Palmer, J.G., Pearson, C., van der Plicht, J., Reimer, R.W., Richards, D.A., Scott, E.M., Southon, J.R., Turney, C.S.M., Wacker, L., Adolphi, F., Büntgen, U., Capano, M., Fahrni, S., Fogtmann-Schulz, A., Friedrich, R., Köhler, P., Kudsk, S., Miyake, F., Olsen, J., Reinig, F., Sakamoto, M., Sookdeo, A., Talamo, S., 2020. The IntCal20 Northern Hemisphere radiocarbon age calibration curve (0–55 cal kBP). Radiocarbon 62. https://doi: 10.1017/RDC.2020.41.

Renberg, I., Brännvall, M.L., Bindler, R., Emteryd, O., 2002. Stable lead isotopes and lake sediments-a useful combination for the study of atmospheric lead pollution history. Sci. Total Environ. 292, 45-54. https://doi.org/10.1016/S0048-9697(02)00032-3

Renzi, M., Montero-Ruiz, I., Bode, M., 2009. Non-ferrous metallurgy from the Phoenician site of La Fonteta (Alicante, Spain): a tudy of provenance. J. Archaeol. Sci. 36, 2584-2596. https://doi.org/10.1016/j.jas.2009.07.016

Richards, G.W. 1985. Fossil Mediterranean molluscs as sea-level indicators. Geol. Magaz. 122, 373-381. https://doi.org/10.1017/S0016756800031812

Rivas-Martínez, S., Rivas-Sáenz, S., 2017. Worldwide Bioclimatic Classification System. Available at: http://www.globalbioclimatics.org/ (accessed 15 January 2017).

Rodríguez-Estrella, T., Navarro, F., Ros, M., Carrión, J., Atenza, J., 2011. Holocene morphogenesis along a tectonically unstable coastline in the Western Mediterranean (SE Spain). Quat. Int. 243, 231-248. https://doi.org/10.1016/j.quaint.2011.07.016

Rohde, K.A., Sandland, R., 1975. Factors influencing clustering in the intertidal snail *Cerithium moniliferum*. Mar. Biol. 30, 2013–215. https://doi.org/10.1007/BF00390743

Rommerskirschen, F., Eglinton, G., Dupont, L., Güntner, U., Wenzel, C., Rullkötter, J., 2003. A north to south transect of Holocene southeast Atlantic continental margin sediments: Relationship between aerosol transport and compound-specific $\delta^{13}C$ land plant biomarker and pollen records. Geochem. Geophys. Geosyst. 4, 1-29. https://doi.org/10.1029/2003GC000541

Schütz, L., Rahn, K.A., 1982. Trace element concentrations in erodible soils. Atmos. Environ. 16, 171-176. https://doi.org/10.1016/0004-6981(82)90324-9

Saynor, M.J., Harford, A., 2010. Pilot study on the separation and physical characterisation of lateritic material from the Ranger project area. Internal Report 579, October, Supervising Scientist, Darwin.

Shah, V.G., Dunstan, R.H., Geary, P.M., Coombes, P., Roberts, T.K., Von Nagy-Felsobuki, E., 2007. Evaluating potential applications of faecal sterols in distinguishing sources of faecal contamination from mixed faecal samples. Water Res. 41, 3691–3700. https://doi.org/10.1016/j.watres.2007.04.006

Shotyk, W, Blaser, P, Grünig, A, Cheburkin, A.K., 2000. A new approach for quantifying cumulative, anthropogenic, atmospheric lead deposition using peat cores from bogs: Pb in eight Swiss peat bog profiles. Sci. Total Environ. 249, 281-295. https://doi.org/10.1016/S0048-9697(99)00523-9

Shotyk, W., Weiss, D., Kramersm J.D., Freim R., Cherbukinm A.K., Gloorm M., Reesem S., 2001. Geochemistry of the peat bog at Etang de la Gruère, Jura Mountains, Switzerland, and its record of atmospheric Pb and lithogenic trace metals (Sc, Ti, Zr, and REE) since 12.370 ^{14}C yr BP. Geochim. Cosmochim. Acta 65, 2337-2360. https://doi.org/10.1016/S0016-7037(01)00586-5

Silliman, J.E., Meyers, P.A., Bourbonniere, R.A., 1996. Record of postglacial organic matter delivery and burial in sediment of Lake Ontario. Org. Geochem. 24, 463-472. https://doi.org/10.1016/0146-6380(96)00041-1

Stanley, J.D., Carlson, R.W., Van Beek, G., Jorstad, T.F., Landau, E.A., 2007. Alexandria, Egypt, before Alexander the Great: a multidisciplinary approach yields rich discoveries. GSA Today 17, 4–10.

Stuiver, M., Reimer, P.J., Reimer, R.W., 2021. CALIB 8.2 [WWW program] at http://calib.org (accessed 27 July 2021).

Switzer, A.D., 2013. Measuring and analyzing particle size in a geomorphic context. In: Shroder, J., Switzer, A.D., Kennedy, D.M. (eds.), Treatise on Geomorphology. Academic Press, San Diego. Methods in Geomorphology vol. 14, pp. 224–242. https://doi.org/10.1016/B978-0-12-374739-6.00385-7

Torres, T., Ramallo, S., Sánchez-Palencia, Y., Ros, M., Ortiz, J.E., Navarro, F., Cerezo, F., Rodríguez-Estrella, T., Manteca, I., 2018. Reconstructing human-landscape interactions in the ancient Mediterranean arbour of Cartagena (Spain). The Holocene 28, 879-894. https://doi.org/10.1177/0959683617752838

Torres, T., Ortiz, J.E., Sánchez-Palencia, Y., Ros, M., Navarro, F., López-Cilla, I., Galán, L.A., Ramallo, S., Rodríguez-Estrella, T., Blázquez, A., 2020. The Pleistocene and Holocene records of the Mazarrón Basin (SE Spain). Quat. Int. https://doi.org/10.1016/j.quaint.2020.03.019.

Triantaphyllou, M., Kouli, K., Tsourou, Th., Koukousioura, O., Pavlopoulos, K., Dermitzakis, M., 2010. Paleoenvironmental changes since 3000 BC in the coastal marsh of Vravron (Attica, SE Greece). Quat. Int. 216, 14-22. https://doi.org/10.1016/j.quaint.2009.08.019

Trincherini, P.R., Domergue, C., Manteca, I., Nesta, A., Quarati P., 2009. The identification of lead ingots from the Roman mines of Cartagena. J. Roman Archaeol. 22, 123–145. https://doi.org/10.1017/S1047759400020626

Ueki, A., Suto, T., 1979. Cellular fatty acid composition of sulfate-reducing bacteria. J. Gen. Appl. Microbiol. 25, 185-196. https://doi.org/10.2323/jgam.25.185

Véron, A., Flaux, C., Marriner, N., Poirier, A., Rigaud, S., Morhange, C., Empereur, J.Y., 2013. A 6000-year geochemical record of human activities from Alexandria (Egypt). Quat. Sci. Rev. 81, 138–147. https://doi.org/10.1016/j.quascirev.2013.09.029

Véron, A., Goiran, J.P., Morhange, C., Marriner, N., Empereur, J.Y., 2006. Pollutant lead reveals the pre-Hellenistic occupation and ancient growth of Alexandria, Egypt. Geophys. Res. Lett., https://doi.org/10.1029/2006GL025824.

Véron, A., Morhange, C., Poirier, A., Angeletti, B., Bertoncello, F. 2018. Geochemical markers of human occupation in the lower Argens valley (Fréjus, France): from protohistory to Roman times. J. Archaeol. Sci. Reports 17, 242-249. https://doi.org/10.1016/j.jasrep.2017.09.028

Villar Vidal, J.A., 1993. Livius, T., Historia de Roma desde su fundación, books XXVI-XXX (English translation and notes), Biblioteca Clásica Gredos, Madrid.

Volkman, J.K., Johns, R.B., Gillan, F.T., Perry, G.J., Bavor Jr., H.J., 1980. Microbial lipids of an intertidal sediment. I. Fatty acids and hydrocarbons. Geochim. Cosmochim. Acta 44, 1133–1143. https://doi.org/10.1016/0016-7037(80)90067-8

Volkman, J.K., Revill, A.T., Holdsworth, D.G., Fredericks, D., 2008. Organic matter sources in an enclosed coastal inlet assessed using lipid biomarkers and stable isotopes. Org. Geochem. 39, 689–710. https://doi.org/10.1016/j.orggeochem.2008.02.014

Vött, A., Brückner, H., Handl, M., Schriever, A., 2006. Holocene palaeogeographies of the Astakos coastal plain (Akarnania, NW Greece). Palaeogeogr. Palaeoclimatol. Palaeoecol. 239, 126-146. https://doi.org/10.1016/j.palaeo.2006.01.015

Weiss, D., Shotyk, W., Cheburkin, A.K., Gloor, M., Reese, S., 1997. Atmospheric lead deposition from 12,400 to ca. 2,000 yrs BP in a peat bog profile, Jura Mountains, Switzerland. Water Air Soil Pollut. 100, 311-324. https://doi.org/10.1023/A:1018341029549

Zheng, Y., Zhou, W., Meyers, P.A., Xie, S., 2007. Lipid biomarkers in the Zoige-Hongyuan peat deposit: Indicators of Holocene climate changes in West China. Org. Geochem. 38, 1927-1940. https://doi.org/10.1016/j.orggeochem.2007.06.012

Tables

Table 1. Correlation coefficients and significant levels (correlations statistically significant at the level of $p < 0.001$ are in bold) for ACL, TAR_{HC}, and P_{aq} indices in SFT core.

	CPI	P_{aq}	TAR_{HC}
ACL	**0.763**	**–0.896**	**0.722**
CPI		**-0.747**	**0.774**
P_{aq}			**–0.616**

Figure captions

Fig. 1. Location of the Cartagena Basin with the position of the core. Adapted from Ortiz et al. (2021).

Fig. 2. Stratigraphic section of the Holocene record of SFT core with the chronological scale and the profile of predominant mineral components, together with the downcore presence of ceramic fragments, charcoal, sedes, phytoclasts, molluscs, ostracodes and foraminifers. The environmental interpretation based on mollusc, ostracode and foraminifer associations is included.

Fig. 3. Concentration of *n*-alkanes (µg/kg), predominant *n*-alkane chain, ACL, TAR_{HC}, P_{aq} index and CPIin SFT core, with the chronological scale, and the identification of the paleoenvironmental episodes. Profiles of stanols content (mg/Kg), coprostanol/24-ethylcoprostanol ratio [c/24-ec] and (coprostanol + epicoprostanol)/ (24-ethylcoprostanol + 24-ethylepicoprostanol) ratio [(c+ec)/(24-ec+24-eec)] were also plotted.

Fig. 4. Downcore plots of total, anthropogenic and lithogenic Pb, Zn and Cu concentrations, with their enrichment factors. Anthropogenic and lithogenic concentrations were calculated following Shotyk et al. (2000) using Ti as a conservative element and data were normalized using the average of elemental concentrations of samples.

Tables Supplementary information

Table 1 Suppmenetary information. Radiocarbon age (yr BP) of selected levels from SFT core and calibrated age (yr cal) converted using the Radiocarbon Calibration Program 8.2 (CALIB 8.2) (Stuiver et al., 2021) with the calibration dataset IntCal20 (Reimer et al., 2020).

Sample No.	Depth (m)	$\delta^{13}C$ (V-PDB)	Conventional age BP	Calibrated BP
CNA5746	2.05	-23.9	235±29	277±85
CNA5747	6.00	-21.2	2004±30	1940±66
CNA5748	9.60	-30.4	2045±31	1990±45

Table 2 Supplementary information. Mean aspartic acid and glutamic acid racemization ratios obtained in ostracode valves from SFT core.

Depth (m)	Ostracode species	D/L Asx	D/L Glx	Age (years)
2.05	*Cypris* sp. (4)	0.096±0.013	0.026±0.020	701±525
2.45	*Cypris* sp. (3)	0.096±0.017	0.054±0.033	732±695
2.70	*Cypris* sp. (4)	0.114±0.014	0.029±0.021	1474±572
2.90	*Cypris* sp. (3)	0.107±0.014	0.027±0.004	1174±583
3.05	*Cypris* sp. (5)	0.097±0.005	0.032±0.022	759±196
3.50	*Cypris* sp. (4)	0.107±0.014	0.027±0.004	1175±583
4.10	*Cypris* sp. (5)	0.123±0.015	0.036±0.004	1852±648
4.30	*C. torosa* (2)	0.110±0.011	0.045±0.030	1305±467
5.20	*C. torosa* (4)	0.117±0.006	0.034±0.006	1582±267
5.40	*C. torosa* (3)	0.129±0.010	0.039±0.002	2079±431
6.00	*C. torosa* (3)	0.120±0.020	0.043±0.007	1718±832
6.20	*C. torosa* (2)	0.123±0.004	0.056±0.032	1851±184
6.40	*C. torosa* (1)	0.126	0.032	1970
7.40	*C. torosa* (4)	0.137±0.011	0.035±0.005	2433±457
7.80	*C. torosa* (2)	0.162±0.006	0.048±0.007	3490±253
7.85	*C. torosa* (5)	0.160±0.018	0.046±0.011	3407±754
8.20	*C. torosa* (1)	0.145	0.030	2782
8.40	*C. torosa* (1)	0.136	0.035	2390
8.50	*C. torosa* (1)	0.139	0.031	2529
8.70	*C. torosa* (2)	0.146	0.038	2790
8.90	*C. torosa* (2)	0.141	0.054	2610
9.05	*C. torosa* (5)	0.142±0.010	0.038±0.008	2635±420
9.15	*C. torosa* (1)	0.172	0.055	3910
9.30	*C. torosa* (1)	0.149	0.045	2930
9.65	*C. torosa* (5)	0.228±0.019	0.065±0.010	6233±776
9.80	*C. torosa* (4)	0.217±0.008	0.052±0.010	5799±331
9.90	*C. torosa* (4)	0.218±0.015	0.056±0.009	5806±645
10.00	*C. torosa* (3) + *Aurila* (1)	0.218±0.022	0.066±0.007	5833±942
10.90	*C. torosa* (3)	0.234±0.013	0.067±0.029	6502±548
11.10	*C. torosa* (2) + *Aurila* (1) + *Cypris* (1)	0.215±0.033	0.075±0.046	5692±1397
11.40	*C. torosa* (2) + *Cypris* (1)	0.232±0.017	0.055±0.007	6407±726
11.90	*C. torosa* (1) + *Loxoconcha* (1)	0.224±0.014	0.054±0.001	6094±568
12.00	*C. torosa* (2) + *Aurila* (1)	0.219±0.015	0.043±0.010	5867±638
12.90	*C. torosa* (2)	0.234±0.003	0.069±0.009	6488±130
14.30	*C. torosa* (4)	0.355±0.026	0.155±0.039	145000±31000
14.50	*C. torosa* (5)	0.358±0.033	0.137±0.041	124000±30000

Figures Supplementary Information

Fig. 1 Supplementary information. Bayesian age-depth models established for the Holocene record of SFT core (between 14.2-9.5 m and 9.5-2.0 m) constructed using the software R-code package “Bacon 2.3.7” (Blaauw and Christen 2011), both after 10000 Markov Chain Monte Carlo iterations. The black line indicates the single best model based on the weighted mean age for each depth, and the grey area shows 95% confidence intervals. Dates were obtained through radiocarbon (Table 1 Supplementary information), and amino acid racemization (Table 2 Supplementary information).

Fig. 2 Supplementary information. Typical chromatograms of *n*-alkanes from selected samples in SFT core. Samples maximized: (A) at high molecular weight *n*-alkanes (C_{31}); (B) at high molecular weight *n*-alkanes (C_{29}); (C) at C_{29} *n*-alkane.

Figure 1

Click here to access/download;Figure;Ortiz et al_Figure 1b.jpg

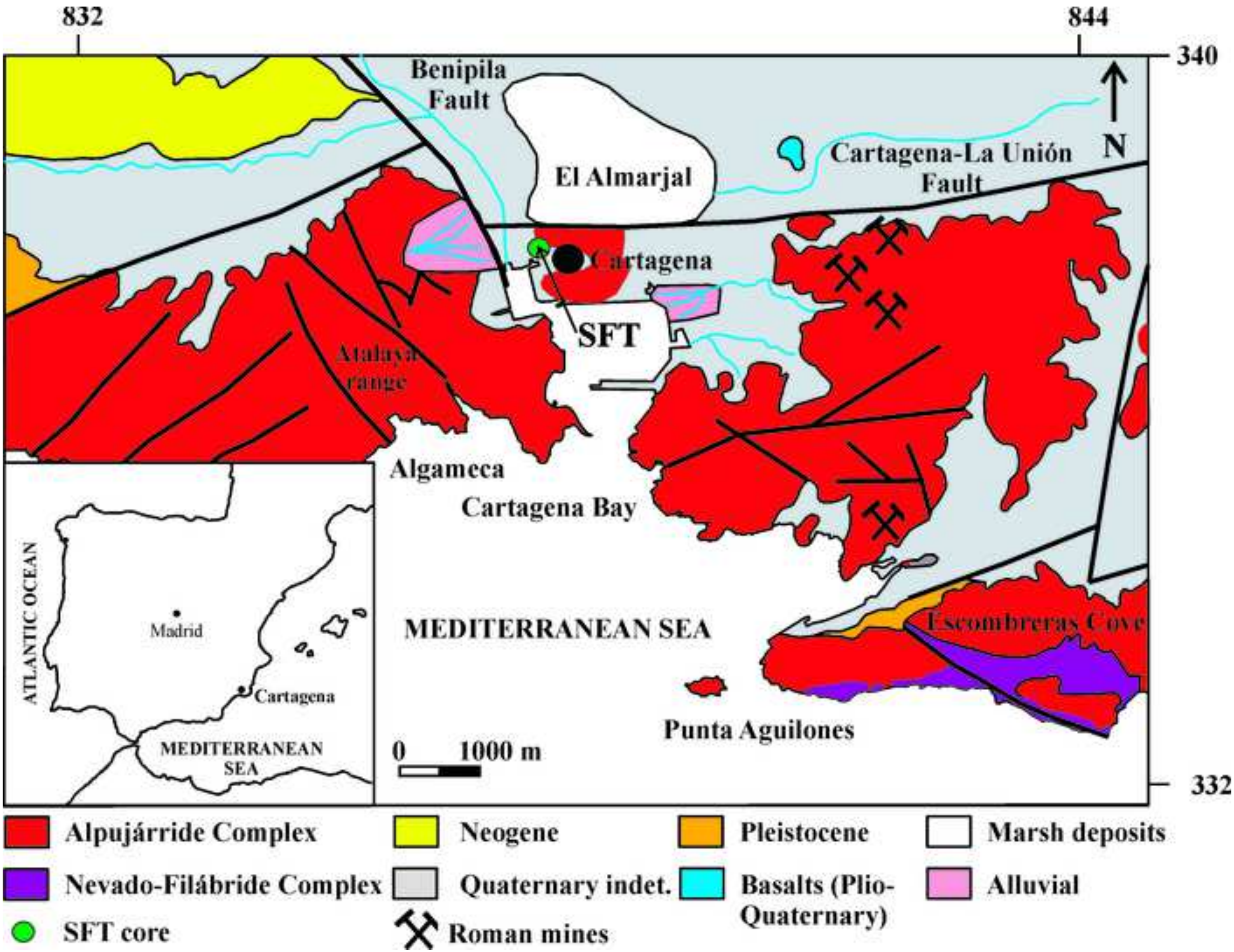

Figure 2

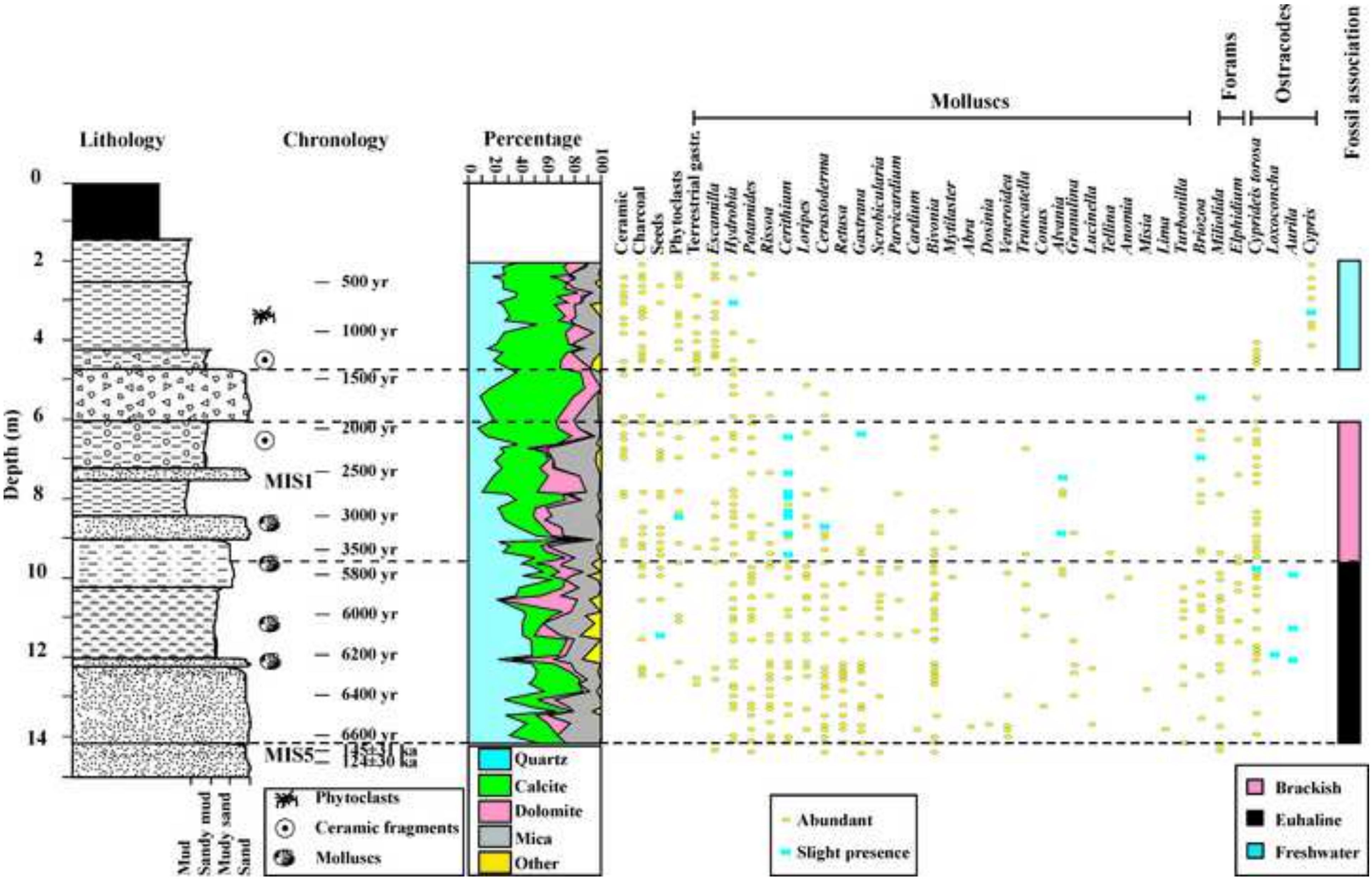

Lithology
Chronology
Percentage
Molluscs
Forams
Ostracodes
Fossil association
Depth (m)
MIS1
MIS5
500 yr
1000 yr
1500 yr
2000 yr
2500 yr
3000 yr
3500 yr
5800 yr
6000 yr
6200 yr
6400 yr
6600 yr
Ceramic
Charcoal
Seeds
Phytoclasts
Terrestrial gastr.
Escamilla
Hydrobia
Potamides
Rissoa
Cerithium
Loripes
Cerastoderma
Retusa
Gastrana
Scrobicularia
Parvicardium
Cardium
Bivonia
Mytilaster
Abra
Dosinia
Veneroidea
Truncatella
Conus
Alvania
Granulina
Lucinella
Tellina
Anomia
Misia
Lima
Turbonilla
Briozoa
Miliolida
Elphidium
Cyprideis torosa
Loxoconcha
Aurila
Cypris
Mud
Sandy mud
Mudy sand
Sand
Phytoclasts
Ceramic fragments
Molluscs
Quartz
Calcite
Dolomite
Mica
Other
Abundant
Slight presence
Brackish
Euhaline
Freshwater

Figure 3

Click here to access/download;Figure;Ortiz et al_Figure 3b.jpg

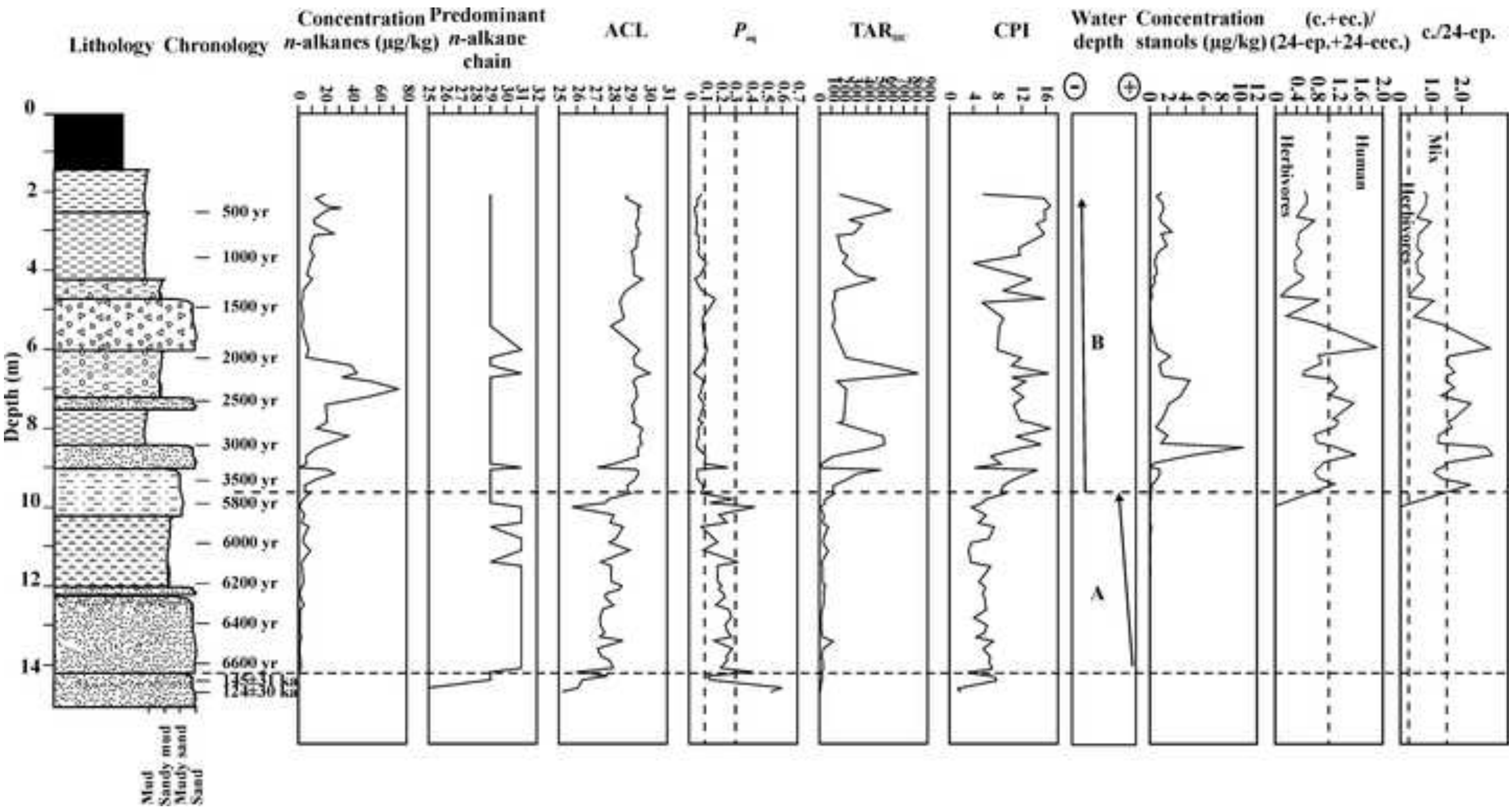

Figure 4

Click here to access/download;Figure;Ortiz et al_Figure 4b.jpg

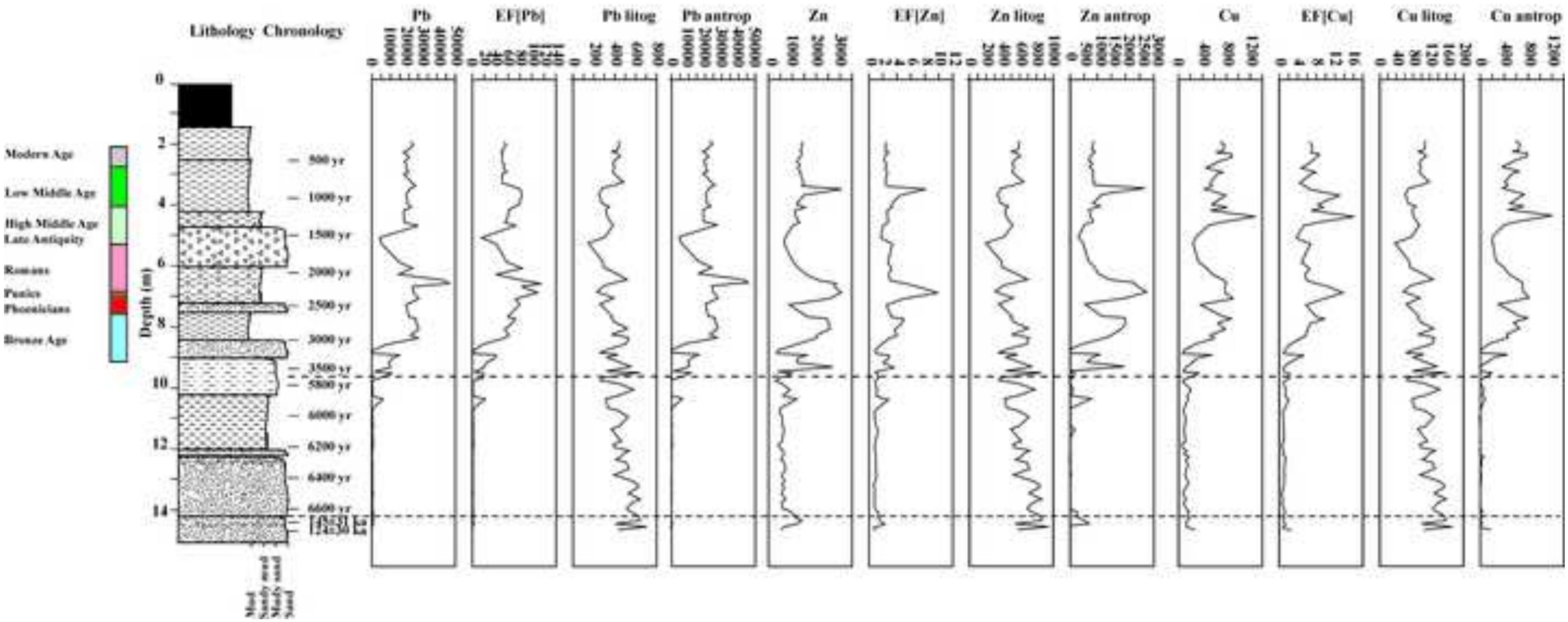

Figure 1 Supplementary Information

Click here to access/download
Supplementary Material
Ortiz et al_Figure 1 SI.jpg

Figure 2 Supplementary Information

Data